Nanotechnology **20** (2009) 375501 (10pp) doi:10.1088/0957-4484/20/37/375501

Carbon nanotubes randomly decorated with gold clusters: from nano^{2}hybrid atomic structures to gas sensing prototypes

J-C Charlier[1], L Arnaud[2], I V Avilov[2], M Delgado[3], F Demoisson[4], E H Espinosa[5], C P Ewels[6], A Felten[2], J Guillot[7], R Ionescu[5], R Leghrib[5], E Llobet[5], A Mansour[7], H-N Migeon[7], J-J Pireaux[2], F Reniers[4], I Suarez-Martinez[6], G E Watson[8] and Z Zanolli[1]

[1] Unité de Physico-Chimie et de Physique des Matériaux (PCPM), European Theoretical Spectroscopy Facility (ETSF), Université Catholique de Louvain, Place Croix du Sud 1, B-1348 Louvain-la-Neuve, Belgium
[2] Centre de Recherche en Physique de la Matière et du Rayonnement (PMR–LISE), Facultés Universitaires Notre-Dame de la Paix, 61 Rue de Bruxelles, B-5000 Namur, Belgium
[3] Sensotran, s.l., Avenida Remolar 31, E-08820 El Prat de Llobregat, Barcelona, Spain
[4] Service de Chimie Analytique et Chimie des Interfaces (CHANI), Université Libre de Bruxelles, Faculté des Sciences, CP255, Boulevard du Triomphe 2, B-1050 Bruxelles, Belgium
[5] Department of Electronic Engineering, Universitat Rovira i Virgili, Avenida Països Catalans 26, E-43007 Tarragona, Spain
[6] Institut des Matériaux Jean Rouxel (IMN), Université de Nantes, 2 rue de la Houssinière–BP 32229, F-44322 Nantes Cedex 3, France
[7] Département Science et Analyse des Matériaux, Centre de Recherche Public–Gabriel Lippmann, rue du Brill 41, L-4422 Belvaux, Luxembourg
[8] The Vega Science Trust, Unit 118, Science Park SQ, Brighton, BN1 9SB, UK[9]

E-mail: jean-jacques.pireaux@fundp.ac.be

Received 10 June 2009, in final form 17 July 2009
Published 26 August 2009
Online at stacks.iop.org/Nano/20/375501

Abstract

Carbon nanotube surfaces, activated and randomly decorated with metal nanoclusters, have been studied in uniquely combined theoretical and experimental approaches as prototypes for molecular recognition. The key concept is to shape metallic clusters that donate or accept a fractional charge upon adsorption of a target molecule, and modify the electron transport in the nanotube. The present work focuses on a simple system, carbon nanotubes with gold clusters. The nature of the gold–nanotube interaction is studied using first-principles techniques. The numerical simulations predict the binding and diffusion energies of gold atoms at the tube surface, including realistic atomic models for defects potentially present at the nanotube surface. The atomic structure of the gold nanoclusters and their effect on the intrinsic electronic quantum transport properties of the nanotube are also predicted. Experimentally, multi-wall CNTs are decorated with gold clusters using (1) vacuum evaporation, after activation with an RF oxygen plasma and (2) colloid solution injected into an RF atmospheric plasma; the hybrid systems are accurately characterized using XPS and TEM techniques. The response of gas sensors based on these nano^{2}hybrids is quantified for the detection of toxic species like NO_2, CO, C_2H_5OH and C_2H_4.

[9] http://www.vega.org.uk.

1. Introduction

Carbon nanotubes (CNTs) have emerged as one of the most exciting nanomaterials, combining a range of extraordinary physical properties, such as extremely small size and high aspect ratio, high stiffness and excellent flexibility under different mechanical stimuli, high structural and chemical stability, and a rich spectrum of electrical properties. Many potential applications have been demonstrated: superstrong composites, energy storage and energy conversion devices, field emission displays, mechanical, chemical and biological probes and sensors, radiation sources, nanoelectronic devices and more [1].

The present paper concentrates on the possibility of using modified CNTs as chemical sensors. Due to their strong sp^2 bonding and near-perfect carbon hexagonal network, pristine carbon nanotubes are not chemically reactive, thus preventing the formation of strong chemical bonds with most molecules. So one wishes to enhance the sensing capability of CNTs by improving their reactivity and sensitivity through functionalization of CNT sidewalls with specific biomolecules or chemical groups [2–5]. Alternatively, metal nanoparticles can be used to decorate CNTs, enabling attachment of other species [6–8]. In such a case, the entire nanoparticle is an integral active part of the sensor, whose detection capability is mainly based on the reactivity of cluster surfaces. Since metal clusters have a broad range of diverse structures (they can, indeed, be produced at different sizes from the nanometre to hundreds of nanometres), they can provide a full range of reactivities for the adsorption of foreign species.

This project [9] focuses on the random decoration of the surface of multi-walled carbon nanotubes (MWCNTs) with metal clusters to tailor the electronic, transport, chemical and sensing properties of the corresponding hybrid nanostructures, hereafter referred to as 'nano^{2}hybrids', in order to reach—within a large field of applications [10–12]—controlled gas sensing properties.

The morphology of the metal coating is dictated by the interactions between the deposited atoms and the CNT surface [13, 14]. For example, a large binding energy between metal atoms and the CNT surface leads to a higher nucleation density and quasi-uniform coverage of the CNT. In the case of titanium that exhibits strong interactions with nanotubes, a homogeneous coating on carbon nanotubes is observed, leading to the formation of nanowires on a nanotube template [13]. However, many types of metals do not form continuous structures on a nanotube surface because of a weaker metal–carbon interaction, thus leading to the formation of isolated metal nanoclusters on the CNT walls. In addition, the interaction between metal atoms, metal clusters and the CNT surface can change if structural and/or chemical defects are present. The density of defects thus plays a key role in the dispersion and resultant size of the metal clusters and can be used to tune their interfacial properties. Consequently, an in-depth understanding of the nature of metal–nanotube interactions is required to obtain functional electronic devices with useful characteristics, but also to propose low resistance ohmic contacts to nanotubes which are crucial to elucidate their intrinsic 1D electronic properties.

In the present work, the interaction between gold nanoclusters and carbon nanotubes has been systematically investigated, using simultaneously both theoretical and experimental approaches. On one side, the gold–nanotube interaction is studied using first-principles techniques. In this framework, numerical simulations have addressed the question of binding and diffusion energies of gold atoms at the tube surface, including realistic atomic models for point defects such as vacancies and di-vacancies. In order to investigate the effect of these gold nanoclusters on the intrinsic properties of the nanotube, both the electronic structures (electronic charge transfer) and the quantum transport were predicted for nanotubes decorated with gold clusters.

On the experimental side, these nano^{2}hybrid systems were synthesized using two different techniques: (1) gold was evaporated from a wire under vacuum conditions onto MWCNTs previously activated with an RF oxygen plasma or (2) the metal nanoparticles from a colloid solution were directly deposited by atmospheric plasma RF mode onto the MWCNTs, without any prior activation of the surface. The nano^{2}hybrids were then spectroscopically and morphologically fully characterized and tested. Transmission electron microscopy (TEM) reveals that the nature and extent of metal coverage can be varied by modifying the plasma pre-treatments of the tube surface. Analyses of the valence band and the core levels by x-ray photoelectron spectroscopy (XPS) reveal poor charge transfer between gold clusters and CNTs.

Gas sensors based on these synthesized nano^{2}hybrid systems were fabricated and tested for their potential in the detection of various toxic species (CO, NO_2, ethanol and ethylene).

2. Understanding the gold–nanotube interaction with a graphene model

A deep understanding of the gold–nanotube interaction is crucial to control the reactivity and gas sensitivity of the nano^{2}hybrid systems. It goes first through the calculation of what happens from the moment a gold atom first hits the surface of a grapheme sheet, used as a model for a carbon nanotube.

Within DFT/LDA calculations, the calculated binding energy of a single gold atom to pristine graphene is 0.73 eV, suggesting that gold will bind to the tube (figure 1). Nonetheless this value is significantly weaker than the binding energy per gold atom in an isolated Au pair (1.39 eV per Au atom). This explains the poor wetting of gold compared to other metals such as Ti, where metal–metal interaction is much stronger than metal–graphene (4.55 eV versus 4.38 eV, respectively); this further suggests gold will preferentially cluster on the carbon nanotube. Indeed, the calculated migration energy of a gold atom on the graphene surface is very low (less than 0.2 eV), suggesting that once isolated gold atoms arrive on the surface they will rapidly migrate. During migration they will encounter either other gold atom(s) or surface defects. The binding energy of Au_2 to pristine graphene is 1.98 eV, higher than that of two isolated Au atoms on the graphene, confirming an extremely strong driving force for clustering.

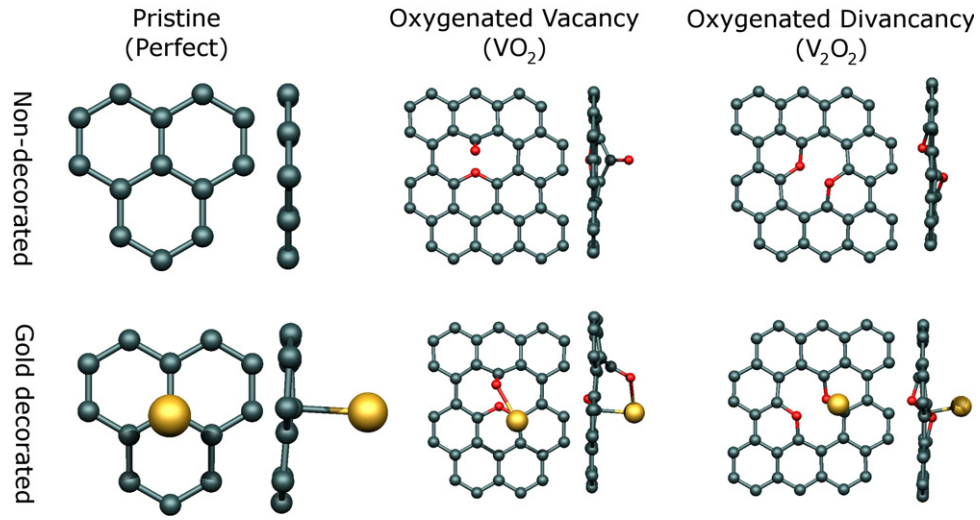

Figure 1. Top and side views of the ground state graphene-like structure obtained within DFT/LDA for non-decorated and single Au atom decorated surfaces.

However, as for most materials, the presence of defects in carbon nanotubes has been demonstrated experimentally [15, 16]. These defects may take different forms: vacancies, adatoms, 'Stone–Wales' defects, pentagon–heptagon pairs, substitution heteroatoms, etc, and are known to modify the electronic properties of the tubes [17]. Rather than viewing defects as an inconvenience, they may provide a way to activate the tube surface and improve gold wetting. Indeed deliberate introduction of defects, or 'active sites', may be a way to overcome the inherent chemical inactivity of carbon nanotube surfaces. With this in mind, the CNTs have been exposed to an oxygen plasma treatment, thus creating vacancies which combine with the oxygen atoms from the plasma [5, 8, 12]. The primary defects are oxygenated vacancies (VO_2) and, to a lesser extent, oxygenated di-vacancies (V_2O_2) (see figure 1) [5].

While a high binding energy is calculated between a gold atom and an undecorated vacancy (3.44 eV), such defects are unlikely to exist since undecorated vacancies are highly reactive, notably in the presence of oxygen (figure 1). Instead, the most common vacancy-related defect will be VO_2, and the DFT/LDA calculations show that a single gold atom binds to VO_2 with an energy of 1.27 eV, i.e. 0.55 eV more than to the pristine surface. This is very close to the 1.39 eV/Au atom binding energy in an isolated gold atom pair. This means that mobile surface Au atoms will be trapped at VO_2, requiring at least over 0.70 eV to migrate away, rendering them immobile until above room temperature. V_2O_2 defects are probably also created by the plasma treatment, and the binding energy of a gold atom to a V_2O_2 defect is very similar to the VO_2 one. Thus these oxygenated vacancy sites created by oxygen plasma treatment (VO_2 and, to a lesser extent, V_2O_2) will act as trapping sites for gold atoms and hence will behave as nucleation sites for gold clusters.

In summary, these first calculations suggest that on untreated tubes gold atoms will rapidly migrate, poorly wet the tubes and form large clusters, whereas in oxygen plasma-treated tubes, gold will bind at oxygen vacancy sites, leading to a more homogeneous size distribution of smaller clusters, because plasma-induced defects will appear randomly on the CNT surface.

A Mulliken population analysis allows us also to investigate the electron distribution for Au bonded to VO_2, showing a net $0.2e^-$ transfer from the gold atom to the defective tube. This is indicative of a potential effect on electron transport, as well as reactivity to gas phase species. Further calculations indeed confirm such an interaction; while they show that an NO_2 molecule binds only very weakly to pristine graphene and VO_2 defects (0.49 eV and 0.39 eV, respectively), this binding energy increases to over 2 eV for the Au–VO_2 complex. In this case, VO_2 sits asymmetrically with one oxygen atom 2.1 Å from the Au one.

While such scoping calculations provide valuable information on the binding energies, structural properties and ground state behaviour of gold atoms, section 3 will investigate the effect of larger gold clusters on the electronic and quantum transport properties of gold decorated nanotubes.

3. Electronic and transport properties of model nanotubes decorated with gold clusters

Within an *ab initio* scheme, the structural, electronic and transport properties of the hybrid system consisting of an Au cluster and ideal CNTs have been investigated. As representative cases of semiconducting and metallic CNTs, an (8, 0) zigzag and a (5, 5) armchair tube have been chosen, respectively. To simulate two possible ways of covering the tube surface, i.e. uniform or 'with particles', both planar (2D) and three-dimensional (3D) cluster shapes have been considered (figure 2). The literature [18] suggests that neutral Au_n clusters with $n \geqslant 12$ have 3D geometry as their lowest-energy isomer. Hence, the Au_{12} cluster was chosen for the present study.

The relative stability and binding properties of the two kinds of clusters on the (8, 0) zigzag tube have been examined. The [tube + 3D cluster] system is 0.137 eV more stable than

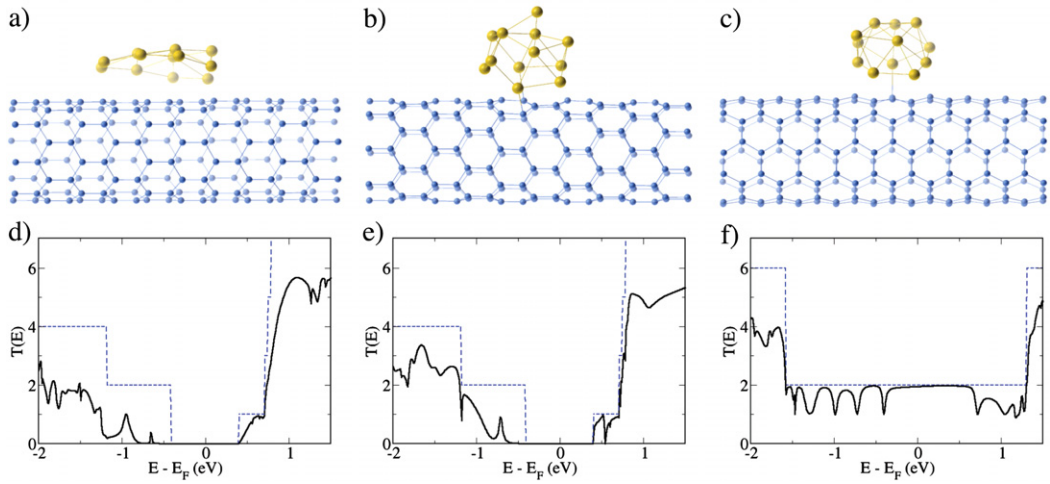

Figure 2. Ball and stick model for nanotubes decorated with various gold clusters: (8, 0) tube with Au_{12} 2D cluster (a), Au_{12} 3D cluster (b) and (5, 5) tube with Au_{12} 3D cluster (c). Corresponding transmission curves for the (8, 0) ((d) and (e)) and (5, 5) (f) tubes are decorated with the Au_{12} cluster. The conductance of the ideal tubes is depicted as a dashed blue line.
(This figure is in colour only in the electronic version)

Table 1. Binding energies of Au_{12} cluster on the (8, 0) zigzag tube and average distance of the nearest gold atoms to the tube within LDA.

$CNT + Au_{12}$ cluster	3D	2D
Binding energy (eV)	3.146	3.178
Average distance (Å)	2.35	3.03

the [tube + 2D cluster]. The average distance between the nearest gold atoms and the nanotube surface was shorter for the 3D than for the 2D cluster, suggesting larger covalent character of the bonding. However, this different bonding character does not result in different metal–tube interactions for the two clusters. Indeed, the binding energy of both clusters to the nanotube (defined as the difference in total energies: $E(Au_{12} + CNT) - E(Au_{12}) - E(CNT)$) is nearly equivalent as summarized, together with the structural parameters, in table 1. The binding energy depends mostly on the Au cluster, not on the chirality of the tube; so the binding energy is expected to be similar in the (5, 5) case. From these calculations, one concludes that, after deposition, the sticking of gold as 3D clusters will be favoured over uniform planar coverage, in agreement with the experimental observations shown in the following sections.

The gas sensing ability of CNTs decorated with metallic clusters relies on a change in conductance (or, equivalently, transmission function) of the latter in the presence of the target gas. Hence, evaluation of the charge transfer between the tube and the metal cluster is a crucial step to be understood in order to select the most promising candidates to construct a working sensor.

Even if the bond between one Au nanocluster and one CNT is not so strong, the resulting charge transfer affects the band structure and hence the conductance of the CNTs. The ideal (8, 0) nanotube is a semiconductor with a gap of ∼0.812 eV (within LDA) while the ideal (5, 5) one is a metal. In the presence of the 2D cluster, the gap of the semiconductor is reduced to 0.709 eV and a state localized on the metal cluster is found at 0.264 eV below the valence band maximum (VBM) (at the Γ point). The interaction of the 3D cluster with the (8, 0) tube leads instead to a reduction of the gap to 0.715 eV and to a state localized on the Au that falls within the gap, at 0.397 eV above the VBM (at the Γ point). In the case of the armchair tube, charge transfer with the 3D cluster leads to the opening of a small gap of 38 meV and to a state localized on the Au at 0.739 eV above the middle point of the gap. The three Au-decorated nanotubes and the corresponding electron transmission curves are illustrated in figures 2(a)–(f).

The calculated transmission functions $T(E)$ show that the conductance around E_F for the three hybrid systems is close to that of the corresponding ideal tubes (dashed lines in figures 2(d)–(f)). In the zigzag tube decorated with the 2D cluster, there is a localized electronic state close to the valence band maximum, which is probably responsible, because of resonant scattering, for a dip in the conductance (figure 2(d)) at the corresponding energy. In the case of the zigzag tube with the 3D cluster, the corresponding localized level lies in the gap (figure 2(e)) and consequently does not strongly influence the conductance as in the 2D case. In contrast, in the armchair case the localized state lies within the conduction band. Its presence is then revealed in the transmission curve by the presence of several dips at various energies (figure 2(f)). Besides some small dips at low energy, the conductance of both zigzag and armchair tubes is almost unaffected by the presence of the gold nanocluster in the energy region close to E_F. This interesting result is promising for gas sensing applications, since the typical experimental energy window for practical use is indeed $[-0.5\text{ eV}, 0.5\text{ eV}]$. Hence, any change in the conductance of the functionalized CNTs in such an energy window will be due exclusively to the presence of the gas to be detected. In other words, the calculated $T(E)$s confirm that gas molecules adsorbed on gold clusters are capable to uniquely modify the conductance of the CNTs, and thus provide a measurable signal.

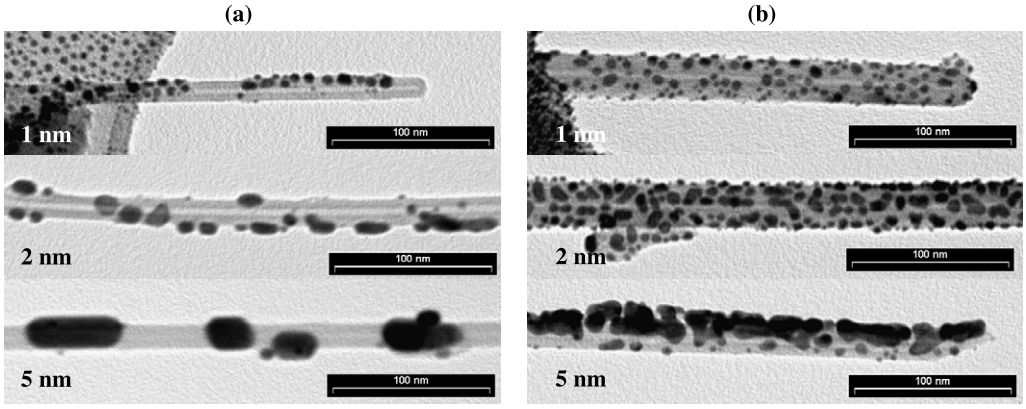

Figure 3. TEM micrographs of different Au coatings on (a) as-received and (b) oxygen-plasma-treated MWCNTs.

4. Synthesis and characterization of nanotubes decorated with gold clusters

According to the predictions of the two previous theoretical sections, the nano^{2}hybrid systems composed of nanotubes decorated with gold nanoclusters have been synthesized and characterized using various specific techniques (TEM, HRTEM and XPS).

In a first set of experiments, oxygen-plasma-treated arc-discharge MWCNTs (powder bought from Mercorp Co.) were decorated with gold clusters. The oxygen plasma treatment was performed using an inductively coupled plasma at an RF frequency of 13.56 MHz. The treatment was performed at a pressure of 0.1 Torr, using a power of 15 W, during 60 s. Figure 3 shows TEM micrographs of the overlayer morphology of an increasing amount of gold evaporated on pristine (a) and oxygen-plasma-treated (b) MWCNTs. In this particular experiment, gold was thermally evaporated simultaneously on both samples in order to guarantee identical amounts of deposited metal, expressed as equivalent thicknesses calibrated using a quartz balance.

Differences in the gold cluster size, shape and distribution can be easily observed. The TEM images recorded on the as-received MWCNTs show that the gold clusters are not uniformly dispersed along the nanotube axis. At 5 nm of coverage, the Au deposition is characterized by large disconnected clusters, leaving sections of the nanotube free of metal coating. This confirms the theoretical results that gold atoms deposited on the nanotube will migrate on the bare surface and merge together to form large clusters; there is only a weak interaction energy between gold atoms and the nanotube surface. Furthermore, using high resolution transmission electron microscopy, it has been shown that Au clusters are preferentially found in regions covered by an amorphous layer [19]. It is thus assumed that the gold nucleation on the CNT surface occurs at defects (in this case an amorphous layer) present at the nanotube surface; as a consequence, the dispersion of the clusters is expected to be random. Therefore it can be postulated that the spatial and size distribution of the clusters can be tuned by deliberately creating defects at the nanotube surface, as also proposed by the *ab initio* calculations.

Oxygen plasma treatment was reported to create structural and chemical defects at the nanotube surface. Photoemission spectroscopy revealed the presence of hydroxyl, carbonyl and carboxylic groups at their surface [5]. Figure 3(b) displays TEM micrographs of gold evaporated on oxygen-plasma-treated MWCNTs. It is observed that gold clusters are more uniformly dispersed compared to deposition on pristine carbon nanotubes. At low metal coverage (1 nm), small and well-dispersed clusters are formed, suggesting that plasma treatment induces reactive sites where gold atoms are easily trapped. At high metal coverage (>5 nm), plasma treatment allows a complete coverage of the nanotube by the metal overlayer. In conclusion, TEM analysis has shown the possibility to change the dispersion and size of the metal nanoparticles on MWCNT surfaces by simply using a plasma pre-treatment and varying the metal evaporation time. Such plasma treatment creates active sites where gold atoms are nucleating, in perfect agreement with the numerical simulations.

Photoemission spectroscopy was also performed on gold-coated nanotubes [20]. The analysis of core level spectra (C 1s, Au 4f) does not show that an Au–C bond is formed; but the Au 4f core level binding energy shifts towards a higher value for the smallest clusters, indicating cluster charging and reduced electronic relaxation during the photoionization process; overall, this suggests poor electrical contact between gold clusters and the CNT surface.

In a second set of experiments, gold particles were directly deposited from a gold colloid solution on MWCNTs by atmospheric plasma treatment. The XPS survey spectrum recorded on the plasma-treated MWCNTs and the fitted core levels of the Au 4f and C 1s peaks are presented in figure 4. The survey spectrum (figure 4(a)) highlights the presence of carbon (at.% 91.6), oxygen (at.% 7.9) and gold (at.% < 1.0), assuming a homogeneous distribution of the elements in the sample and no matrix effects. As the amount of gold was similar after a washing in ethanol solution, this result suggests a strong adhesion of the gold nanoparticles onto the multi-wall CNTs. The Au 4f spectrum (figure 4(b)) is unambiguously assigned to metallic gold [21, 22]. In order to distinguish the oxygen functional groups [23], the C 1s spectra (figure 4(c)) have been fitted to five line curves with binding energies at

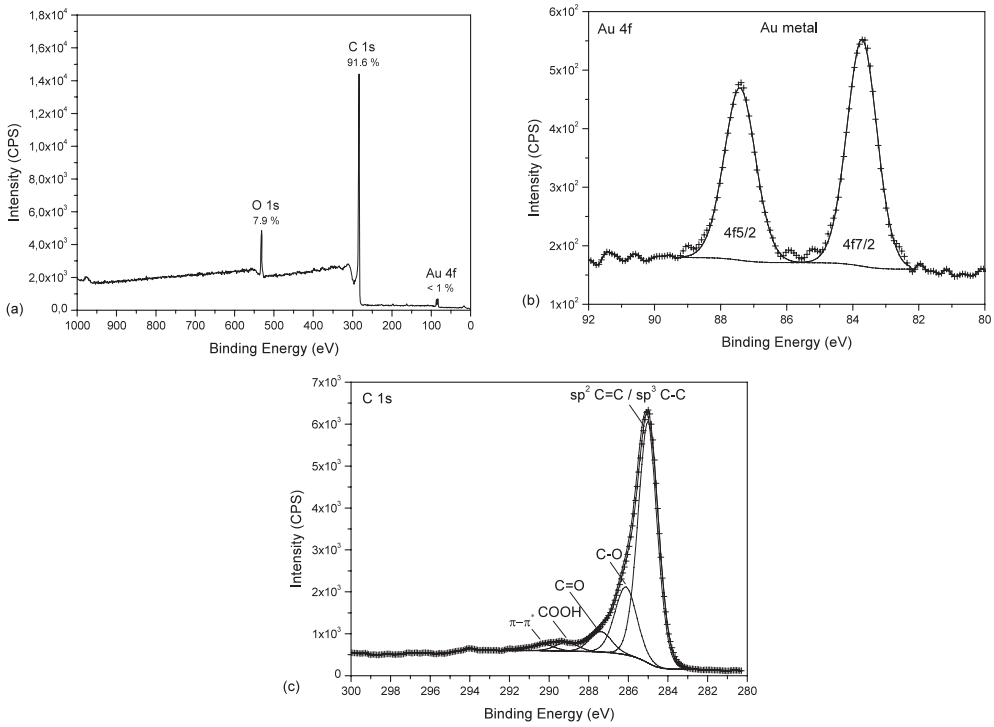

Figure 4. XPS spectra recorded on MWCNTs after atmospheric Ar plasma treatment [27]: (a) survey spectrum, (b) fitted Au(4f) core level and (c) fitted C(1s) core level.

284.9, 286.2, 287.4, 288.8 and 290.9 eV, using a fixed FWHM of 1.3 eV [24]. These binding energy peaks are assigned to sp^2 C=C/sp^3 C–C, C–O, C=O, COOH and π–π^* shake-up, respectively. The presence of the carbon–oxygen species was expected since the sample was exposed during plasma treatment to a strong oxidizing atmosphere due to the injection of water droplets. Indeed, optical emission spectrometry of the post-discharge reveals the presence of atomic oxygen lines at 777 and 852 nm. The presence of oxygen on the surface is also expected from the theoretical model (see previous sections), which indicates that bound oxygen—as chemical and/or structural local defects—promotes the binding of Au to the surface.

We have ascertained that no large scale structural damages are brought to the MWCNTs (leading to the modification of their properties) [25] from the plasma treatment process. Figure 5(a) shows a high resolution TEM image of MWCNTs after the Ar plasma treatment. The nanotubes often appeared with a smooth surface with a well-preserved graphene-layer structure, in agreement with the literature data concerning the effects of the plasma treatment on CNTs [25, 26]. Figure 5(b) shows a typical TEM image of MWCNTs covered with gold metallic nanoclusters obtained after the atmospheric Ar plasma treatment [27]. Most of the nanotubes are isolated and nearly no carbon nanoparticle agglomeration is observed. Note that the 10 nm diameter of the spherical Au metal clusters is similar to the one of the gold colloid solution. Similar results have been obtained on highly oriented pyrolitic graphite (HOPG) substrates [28]. In agreement with XPS results (figure 4), the small amount of deposited gold (<1.0 at.%) is to be related to the existence of a small number of oxygen-containing groups on the MWCNT surface (8 at.%.). However, the deconvolution of the Au XPs peak, using the Quases–Tougaard software, for HOPG samples, submitted to the same plasma treatment, reveals that the 1% Au concentration corresponds to a surface coverage of approximately 10% [28].

Table 2. Average responsiveness (and standard deviation) of the Au-decorated MWCNTs sensors towards the various toxic species tested.

Species	Concentration (ppb)	SR % (25 °C)	SR % (150 °C)
NO_2	500	6.50 (0.52)	4.20 (0.50)
	1 500	9.40 (0.70)	7.40 (0.68)
	6 500	12.00 (0.79)	12.40 (0.81)
CO	50 000	1.00 (0.13)	0.90 (0.14)
Ethanol	50 000	0.44 (0.06)	0.48 (0.08)
Ethylene	50 000	0.08 (0.02)	0.11 (0.04)

5. Fabrication of gas sensors based on nanotubes decorated with gold clusters

In order to investigate the sensing properties of these hybrids composed of nanotubes decorated with gold nanoclusters, gas sensors have been fabricated and their sensitivity to various toxic gases investigated.

The average responsiveness of the sensors (SR) over four replicated measurements is summarized in table 2. The results indicate that the Au-decorated MWCNTs are sensitive to NO_2, even when operated at room temperature, with a responsiveness up to 6% for as low as 500 ppb, which rises to 12% for 6.5 ppm of NO_2.

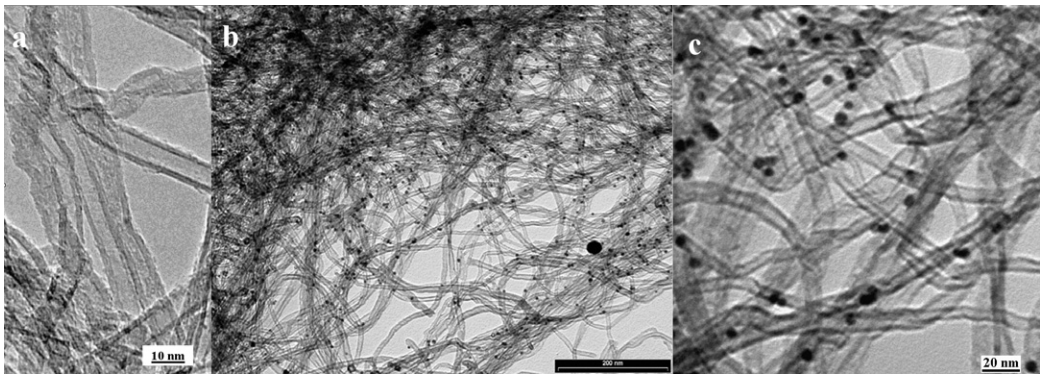

Figure 5. TEM micrographs of MWCNTs: (a) high resolution image of Ar plasma-treated MWCNTs showing no structural damage before gold deposition, (b) low magnification image (reproduced from [27] with permission of F Reniers) and (c) high magnification image of MWCNTs covered with gold metallic nanoclusters (10 nm) deposited by atmospheric Ar plasma treatment. Scale bars are 10, 200 and 20 nm on (a), (b) and (c), respectively.

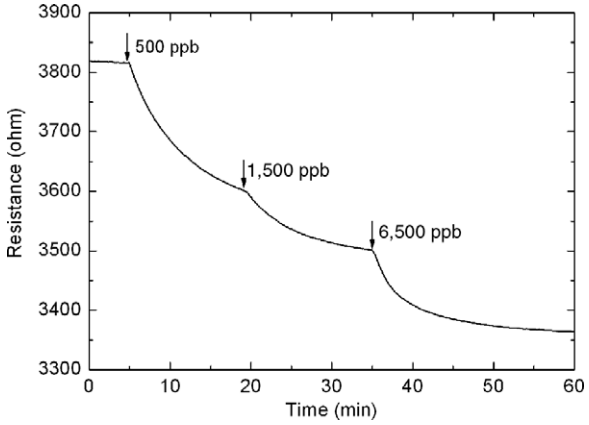

Figure 6. Resistance change experienced by Au-decorated MWCNT sensor operated at ambient temperature to successive injections of NO_2.

A typical response curve for NO_2 detection is shown in figure 6. When operated at room temperature, the sensor needed approximately 20 min to reach a steady state resistance value after gas injection. Although the response time could be reduced by almost a factor of two when operating the sensor at 150 °C, its sensitivity was not better than at ambient temperature. The behaviour of the gas-sensitive films was similar to a p-type semiconductor, as their resistance decreased in the presence of NO_2 (i.e. an oxidizing species).

Regarding the detection at ambient temperature of the other studied vapours, sensor responsiveness was near 1% for 50 ppm of CO, 0.44% for 50 ppm of ethanol and 0.08% for 50 ppm of ethylene. With such low responsiveness to these species, it can be deduced that the Au-decorated MWCNT sensors are able to selectively detect NO_2 at the operating temperatures tested. The presence of CO, ethanol or ethylene at levels of tens of ppm would not cause serious interference to the detection of NO_2 at ppb levels. At present, the commercially available sensors have sensitivities in the ppm range; the ppb level can only be reached with analysers. Commercial sensors both for safety, hygiene or environmental purposes have ranges between 0–200 and 0–1000 ppm. The nano^{2}hybrid-based sensors open a promising future for environmental analyses because of the need to measure in the ppb range, but the response time needs to be reduced. No standards have been agreed upon for nitrogen oxides in indoor air but, ASHRAE and the US EPA National Ambient Air Quality Standards list 53 ppb as the average 24 h limit for NO_2 in outdoor air.

6. Conclusion

In the present work, first-principles theoretical techniques have been used to investigate the nature of gold–carbon nanotube interactions. The calculations reveal that this interaction is quite weak, allowing Au migration at the nanotube surface. Defects (or 'active sites') such as oxygenated vacancies or di-vacancies may trap these diffusive Au atoms and play the role of nucleation centres for a future gold cluster, which will be stabilized by the stronger Au–Au interaction.

The successful synthesis and the characterization of the nano^{2}hybrid system based on multi-wall nanotubes randomly decorated with gold clusters corroborate these predictions. Indeed, TEM images demonstrate the possibility to control the spatial dispersion and size of the metal nanoparticles on multi-wall CNT surfaces by simply varying the metal evaporation time and by using a plasma pre-treatment that deliberately creates defects at the nanotube surface. The use of colloidal gold precursors provides another route for precise control of metal nanoparticle size.

In addition, both the electronic and transport properties of the carbon nanotubes have been predicted to be only slightly affected by charge transfer from the gold cluster. This renders these nano^{2}hybrid systems promising candidates for gas sensing since this intrinsic mechanism relies on the change in conductance in the presence of the gas to be sensed. As predicted theoretically for nanotubes decorated with aluminium clusters [7], electron transport in the nanotube is affected by very small charge transfer values: 0.1 electrons per molecule are sufficient for its detection.

The sensing properties of the nano^{2}hybrid gas sensors have been quantified, and these Au-decorated multi-wall CNT

sensors are found to selectively detect NO_2 at room and 150 °C temperatures. Although their response time is of the order of several minutes, they are reusable for sensing, thanks to the small adsorption energy.

In conclusion, the hybrid systems, represented here by the prototypical composite—multi-wall CNTs randomly decorated by gold nanoclusters (nano^{2}hybrids)—are indeed promising systems for the design of novel molecular sensors. In addition, given the great flexibility in functionalization of metallic clusters, these nano^{2}hybrid systems could be tailored for recognition of specific chemical agents with high selectivity and specificity. Although still at the 'proof-of-principle' stage, the CNT–metal cluster architecture might provide a promising and important avenue for the development of nanoscale sensing devices.

7. Experimental details

7.1. Understanding the gold–nanotube interaction with a graphene model

Density functional theory (DFT) [29] has been used within the local density approximation (LDA) [30] as coded in the AIMPRO package [31]. The calculations used large supercells, fitting the charge density to plane waves within an energy cutoff of 200 Ryd. Charge density oscillations in partly filled degenerate orbitals during the self-consistency cycle were damped using a Fermi occupation function with $k_BT = 0.04$ eV. Atom-centred Gaussian basis functions are used to construct the many-electron wavefunction. These functions are labelled by four orbital symbols, where for each symbol all angular momenta are allowed up to maxima p ($l = 0, 1$) and d ($l = 0, 1, 2$), respectively. Following this nomenclature, the basis sets pdddp and dddd are used for C and Au, respectively. A Bloch sum of these functions is performed over the lattice vectors to satisfy the periodic boundary conditions of the supercell. Calculations were performed on an $8 \times 8 \times 1$ unit cell of graphene containing 128 C atoms, with Brillouin zone sampling $1 \times 1 \times 1$ k-points within the Monkhorst–Pack scheme [32]. It was verified that these k-points converge energies within 0.002 au. In the analysis that follows, a perfect layer of graphene and isolated metal atom were taken as the standard reference states of carbon and metal, respectively.

7.2. Electronic and transport properties of model nanotubes decorated with gold clusters

The (gold nanocluster + nanotube) atomic structure has been studied and ground state electronic calculations have been performed using DFT [29] under the LDA [30] for the exchange–correlation functional, as implemented in the SIESTA code [33]. Norm-conserving Troullier–Martin pseudopotentials in the Kleinman–Bylander non-local form [34] have been constructed for both the 11 valence electrons of Au (relativistic) and the 4 valence electrons of C. Numerical pseudo-atomic orbitals have been used as the basis set to expand the wavefunctions. A double-ζ basis set has been used for the s and p states of C, while for Au a double-ζ polarized for the s states and double-ζ for the d states has been used. The Brillouin zone has been sampled by 4 k-points (Γ-point included) generated according to the Monkhorst–Pack scheme [32]. The Fermi–Dirac function with a smearing temperature of 300 K was used to define the occupation of the electronic states. These values and a kinetic energy cutoff of 200 Ryd were enough to converge the electronic properties of the system. The cell size along the directions perpendicular to the tube axis was fixed to 20 Å. To avoid gold cluster–cluster interactions, the number of repetitions of the unit cell of the ideal CNT has been chosen large enough to ensure a distance between cluster images of at least 15 Å. This leads to five cells and nine cells in the zigzag and armchair case, respectively, which is a repetition unit consisting of 172 and 192 atoms. The atomic positions and cell size along the tube axis have been fully relaxed via the conjugate gradient method until the forces on the ions were less than 0.01 eV Å^{-1}.

In order to evaluate the charge transfer between the tube and the metal cluster an algorithm [35] based on the Bader decomposition [36] of the electronic charge density of a complex system into atomic contributions has been employed. Charge transfer between the tube and the metallic cluster occurs in opposite directions depending on whether the Au cluster is 2D or 3D. The interaction of the 2D cluster with an (8, 0) zigzag tube leads to an excess charge on the gold of 0.065 q_e (where q_e is the absolute value of the electron charge) while in the 3D case, a charge of 0.108 and 0.238 q_e is transferred to the (5, 5) and (8, 0) tubes, respectively.

The transport calculations have been performed within the non-equilibrium Green function (NEGF) [37] formalism using the first-principles Hamiltonian of the SIESTA calculation, as implemented in the SMEAGOL code [38]. The system studied in the transport problem consists of a central 'device' and two 'leads' regions. The device consists of a tube segment made from five (zigzag) or nine (armchair) cells (±22 Å in length) with the gold cluster. As contacts, two cells of ideal CNTs were used, since we are interested in the change of the transmission properties of the tube exclusively due to the presence of the Au cluster. The transport calculations were performed at the Γ-point. The kinetic energy cutoff was raised to 400 Ryd to ensure a good sampling of the Hartree potential.

7.3. Synthesis and characterization of nanotubes decorated with gold clusters, first experiment

The oxygen plasma treatment was performed using inductively coupled plasma at an RF frequency of 13.56 MHz [5] with a power of 15 W, under a pressure of 0.1 Torr. Treatment time was 60 s. Gold was then thermally evaporated from a gold wire. A quartz microbalance was used to measure *in situ* the quantity of metal evaporated onto the CNT samples. The nanotubes were dispersed in ethanol, and a drop was deposited onto a lacey carbon film supported by a copper grid. Transmission electron microscopy was carried out using a Philips Tecnai 10 microscope operating at 80 kV (to limit electron beam damage) and a LEO 922 OMEGA (LaB_6 electron source) operating at 200 kV (point resolution of 0.29 nm).

7.4. Synthesis and characterization of nanotubes decorated with gold clusters, second experiment

MWCNTs were soaked in ethanol for up to 15 min before each experiment. The gold colloidal solution was prepared by the citrate thermal reduction method, resulting in a stable dispersion of gold particles ([Au] = 134 mM) with an average diameter of around 10 nm and 10% poly-dispersity. The nano^{2}hybrid devices have been prepared by spraying the gold colloid solution into the post-discharge of a plasma; the plasma generator is an Atomflo™ -250 plasma source from Surfx Technologies LLC [39]. This method has already been successfully used to deposit 10 nm gold on HOPG surfaces [28]. The plasma activation and deposition process is described in [27]. A magnet was used to stir the MWCNTs during the plasma treatment. After plasma treatment, the resulting nanomaterials were plunged into an ethanol solution for 5 min and were submitted to ultrasonication before experimental characterization. In order to evaluate their chemical composition by XPS, the samples were pressed onto a Cu tape; charging effects on the measured binding energy positions were corrected by setting the binding energy component of the Au 4f (7/2) peak to 83.7 eV.

7.5. Fabrication of gas sensors based on nanotubes decorated with gold clusters

Silicon-based micro-hotplate sensor substrates (CNM, Barcelona) [40] have been used to test the gas sensing properties of the Au-decorated MWCNTs. The deposition of the sensing material was performed by the drop coating method using a microinjector (JBE1113 Dispenser, I&J FISNAR Inc., USA). As the metal-decorated nanotubes are polar, a polar organic vehicle has been employed to better disperse the nanotubes. Thus, the deposition paste was prepared by dispersing the CNTs in glycerol (700 mg ml^{-1}). The dispersion and adequate mixture of the components were further enhanced by stirring the solution in an ultrasonic bath at 75 °C for 2 h. The deposited films were dried at 170 °C for 1 h in order to burn out the organic vehicle and finally annealed at 400 °C for 2 h. These processes were carried out in air atmosphere, and ensured a good adherence of the sensing material to the sensor substrates. Gas sensing tests were run to investigate the detection of various toxic species (CO, NO_2, ethanol and ethylene). The sensors were operated both at room temperature and at 150 °C. During the measurements, the sensors were kept inside a 5.3 cm^3 test chamber, and different concentrations of each gas species were introduced by the direct injection method using a gas-tight chromatographic syringe. After each series of successive injections, the sensor chamber was flushed with pure dry air for 1 h, while the sensors were kept heated at 150 °C to speed up gas desorption. Finally, the airflow was interrupted and the sensors were left at ambient temperature during 12 h, which ensured full recovery of their baseline resistance. The performance of these Au-decorated MWCNT sensors was quantified in terms of the resistance change due to its exposure to a test gas and the sensor baseline resistance in air:

$$\mathrm{SR} = \frac{(R_{\mathrm{air}} - R_{\mathrm{gas}})}{R_{\mathrm{air}}} \times 100(\%)$$

where SR defines sensor responsiveness, and R_{air} and R_{gas} are the sensor resistance in air and in the presence of a toxic species, respectively. Each measurement was replicated four times in order to assess the reproducibility of the results.

Acknowledgment

This work was supported by the EU-STREP project Nano2hybrids (no. 033311).

References

[1] Jorio A, Dresselhaus G and Dresselhaus M S 2008 *Carbon Nanotubes* (*Topics in Applied Physics*) (Berlin: Springer) p 111
[2] Wong S S, Joselevich E, Woolley A T, Cheung C and Lieber C M 1998 *Nature* **394** 52
[3] Chen R J, Zhang Y, Wang D and Dai H 2001 *J. Am. Chem. Soc.* **123** 3838
[4] Besteman K, Lee J-O, Wiertz F G M, Heering H A and Dekker C 2003 *Nano Lett.* **3** 727
[5] Felten A, Bittencourt C, Pireaux J J, Van Lier G and Charlier J C 2005 *J. Appl. Phys.* **98** 074308
[6] Kong J, Chapline M G and Dai H 2001 *Adv. Mater.* **13** 1384
[7] Zhao Q, Buongiorno Nardelli M, Lu W and Bernholc J 2005 *Nano Lett.* **5** 847
[8] Bittencourt C, Felten A, Douhard B, Colomer J F, Van Tendeloo G, Drube W, Ghijsen J and Pireaux J J 2007 *Surf. Sci.* **601** 2800
[9] http://www.nano2hybrids.net/ Progress in the development of new gas sensing devices based on hybrid nanomaterials are regularly posted on the project website (all feedback is welcome!). Short videos giving further background information to the project can also be viewed at http://www.vega.org.uk
[10] Kong J, Franklin N R, Zhou C W, Chapline M G, Peng S, Cho K J and Dai H 2000 *Science* **287** 622
[11] Collins P G, Bradley K, Ishigami M and Zettl A 2000 *Science* **287** 1801
[12] Ionescu R *et al* 2006 *Sensors Actuators* B **17** 36
[13] Zhang Y, Franklin N W, Chen R J and Dai H 2000 *Chem. Phys. Lett.* **331** 35
[14] Zhang Y and Dai H 2000 *Appl. Phys. Lett.* **77** 3015
[15] Hashimoto A, Suenaga K, Gloter A, Urita K and Iijima S 2004 *Nature* **430** 870
[16] Koshino M, Sato Y, Urita K and Iijima S 2007 *Nat. Nanotechnol.* **2** 358
[17] Charlier J-C 2002 *Acc. Chem. Res.* **35** 1063
[18] Fernández E M, Soler J M, Garzón I L and Bálbas L C 2004 *Phys. Rev.* B **70** 165403
[19] Felten A, Bittencourt C, Colomer J-F, Van Tendeloo G and Pireaux J-J 2007 *Carbon* **45** 110
[20] Bittencourt C, Felten A, Douhard B, Ghijsen J, Johnson R L, Drube W and Pireaux J-J 2006 *Chem. Phys.* **328** 385
[21] Briggs D and Seah M P 1990 Practical surface analysis *Auger and X-ray Photoelectron Spectroscopy* 2nd edn, vol 1 (New York: Wiley)
[22] Buttner M and Oelhafen P 2006 *Surf. Sci.* **600** 1170
[23] Paredes J I, Martinez-Alonso A and Tascon J M D 2007 *Langmuir* **23** 8932
[24] He X, Zhang F, Wang R and Liu W 2007 *Carbon* **45** 2559
[25] Yuxiang Q and Ming H 2008 *Appl. Surf. Sci.* **254** 1757
[26] Samukawa S, Ishikawa Y, Okumura K, Sato Y, Tohji K and Ishida T 2008 *J. Phys. D: Appl. Phys.* **41** 024006
[27] Reniers F, Demoisson F and Pireaux J J 2007 Procédé de dépôt de nanoparticules sur un support *Patent* 14.08.07/EPA 07114344

[28] Demoisson F, Raes M, Terryn H, Guillot J, Migeon H-N and Reniers F 2008 *Surf. Interface Anal.* **40** 566
[29] Hohenberg P and Kohn W 1964 *Phys. Rev.* **136** B864
Kohn W and Sham L J 1965 *Phys. Rev.* **145** 561
[30] Ceperley D M and Alder B J 1980 *Phys. Rev. Lett.* **45** 566
[31] Briddon P R and Jones R 2000 *Phys. Status Solidi* b **217** 131
[32] Monkhorst H J and Pack J D 1976 *Phys. Rev.* B **13** 5188
[33] Soler J M, Artacho E, Gale J, Garcia D A, Junquera J, Ordejón P and Sánchez-Portal D 2002 *J. Phys.: Condens. Matter* **14** 2745
[34] Kleinman L and Bylander D M 1982 *Phys. Rev. Lett.* **48** 1425
[35] Henkelman G, Arnaldsson A and Jónsson H 2006 *Comput. Mater. Sci.* **36** 354
[36] Bader R 1990 *Atoms in Molecules: A Quantum Theory* (New York: Oxford University Press)
[37] Datta S 1995 *Electronic Transport in Mesoscopic Systems* (Cambridge: Cambridge University Press)
[38] Rocha A R, García-Suárez V M, Bailey S W, Lambert C J, Ferrer J and Sanvito S 2006 *Phys. Rev.* B **73** 085414
[39] Ladwig A, Babayan S, Smith M, Hester M, Highland W, Koch R and Hicks R 2007 *Surf. Coat. Technol.* **201** 6460
[40] Rickerby D G, Wätchter N, Horrillo M C, Gutiérrez J, Gràcia I and Cané C 2000 *Sensors Actuators* B **69** 314